

studies. Figure 4B shows the SWNT tangential modes recorded using a micro-Raman spectrometer (DILOR XY) in back-scattering geometry and VV configuration (same polarization for the incident and scattered light). The polarized 514 nm incident laser was focused by a 10× microscope objective to 100 μm diameter spot size. The intensities of the SWNT tangential mode decreased with increasing sample rotation angle (at 0°, the laser polarization direction is parallel to the sample alignment direction). The angular dependence of the relative intensities of SWNT tangential modes measured from the macroscopic samples is similar to the published result obtained from a microscopic sample comprising a few aligned SWNT bundles,<sup>[8,9]</sup> confirming that the self-assembled SWNT films are highly ordered.

Under a polarized optical microscope, the macroscopic SWNT films showed birefringence, with extinction at 0° (nanotube alignment direction parallel to the polarization direction) and 90° and maximum transparency at 45° over the entire surface area (Figs. 4C,D). The result is consistent with the expected anisotropic polarizability of the individual carbon nanotubes and demonstrates long-range orientational ordering of these materials. Preliminary transport measurements performed on thick films show that, similar to the results from the magnetically aligned nanotube ribbons,<sup>[10]</sup> the electrical conductivity of the self-assembled SWNT film is substantially higher parallel than perpendicular to the alignment direction.

The hydrophilic nature of etched SWNT bundles is attributed to the presence of sidewall defects created by chemical etching. High-resolution TEM studies show that the surfaces of the SWNT bundles become rugged and are often coated with a thin layer of amorphous carbon after etching. Similar to the dangling bonds on the opened ends, these sidewall defects are likely to be terminated by polar groups that make the nanotube hydrophilic. The etched SWNTs can no longer be dispersed in water if vacuum annealed at temperatures above 400 °C, a condition known to “heal” the defects on the graphene shells.<sup>[11]</sup> Our HRTEM measurements show that the clear and smooth lattice fringes of the SWNTs re-appeared after annealing at 400 °C in 10<sup>-6</sup> torr vacuum, which is below the melting temperature of the glass substrate.

We propose that self-assembly of SWNTs on solid substrates is due to heterogeneous nucleation of nanotubes from a locally super-saturated suspension. When a hydrophilic substrate was immersed into a stable suspension with a nanotube concentration  $C_0$  less than a critical concentration  $C^*$ , no deposition occurred initially although the suspension wetted the substrate (Fig. 2). With gradual evaporation of the water, the overall nanotube concentration increased. Under non-equilibrium conditions, the local nanotube concentration in the meniscus area,  $C_M$ , should be much higher than the overall concentration  $C$ . If the initial concentration  $C_0$  is close to  $C^*$  and the evaporation rate is sufficiently high,  $C_M$  can exceed  $C^*$ , which results in precipitation of the CNTs from the suspension. The results reported here indicate that heterogeneous nucleation on hydrophilic surfaces is energetically more

favorable than homogeneous nucleation. If  $C_0$  is substantially smaller than  $C^*$ , it is likely that  $C_M < C^*$  even at a high evaporation rate, in which case no deposition of CNTs should occur. This is consistent with the experimental observation that no SWNTs transferred to the glass slide when  $C_0 < 0.1 \text{ g L}^{-1}$ . This mechanism is in essence the classic heterogeneous nucleation process<sup>[12]</sup> and is similar to the one proposed for self-assembly of nanocomposites via selective solvent evaporation.<sup>[3]</sup>

Similar to the case of nematic liquid crystals and Langmuir–Blodgett films, the driving force for ordering is attributed to maximizing the van der Waals interaction between the near-neighbor CNTs. The dimension of the etched SWNT bundles is in fact similar to some of the large virus molecules known to form liquid crystal phases. It is likely that alignment was also assisted by the surface tension at the interface between water and the hydrophilic substrate. Such forces are known to contribute to the alignment of large organic molecules such as DNA strands under similar conditions.<sup>[4]</sup>

Received: January 25, 2002  
Final version: April 2, 2002

- [1] A. Ulman, *An Introduction to Ultrathin Organic Films: From Langmuir–Blodgett to Self-Assembly*, Academic Press, San Diego, CA 1991.
- [2] Y. A. Vlasov, X. Z. Bo, J. C. Sturm, D. J. Norris, *Nature* **2001**, 414, 289.
- [3] Y. Lu, Y. Yang, A. Sellinger, M. Lu, J. Huang, H. Fan, R. Haddad, G. Lopez, A. R. Burns, D. Y. Sasaki, J. Shelnut, C. J. Brinker, *Nature* **2001**, 410, 913.
- [4] A. Bensimon, A. Simon, A. Chiffaudel, V. Croquette, F. Heslot, D. Bensimon, *Science* **1994**, 265, 2096.
- [5] X. P. Tang, A. Kleinhammes, H. Shimoda, L. Fleming, C. Bower, S. Sinha, O. Zhou, Y. Wu, *Science* **2000**, 228, 492.
- [6] J. Liu, A. Rinzler, H. Dai, J. Hafner, A. R. Bradley, P. Boul, A. Lu, T. Iverson, A. K. Shelimov, C. Huffman, F. Rodriguez-Macias, Y. Shon, R. Lee, D. Colbert, R. E. Smalley, *Science* **1998**, 280, 1253.
- [7] H. Shimoda, B. Gao, X. P. Tang, A. Kleinhammes, L. Fleming, Y. Wu, O. Zhou, *Phys. Rev. Lett.* **2002**, 88(1), 15 502.
- [8] H. H. Gommans, J. W. Alldredge, H. Tashiro, J. Park, J. Magnuson, A. G. Rinzler, *J. Appl. Phys.* **2000**, 88, 2509.
- [9] C. Fantini, M. A. Pimenta, M. S. S. Dantas, D. Ugarte, A. M. Rao, A. Jorio, G. Dresselhaus, M. S. Dresselhaus, *Phys. Rev. B* **2001**, 63, 161 405(R).
- [10] B. W. Smith, Z. Benes, D. E. Luzzi, J. E. Fischer, D. A. Walters, M. J. Casavant, J. Schmidt, R. E. Smalley, *Appl. Phys. Lett.* **2000**, 77, 663.
- [11] B. W. Smith, D. E. Luzzi, *Chem. Phys. Lett.* **2000**, 321, 169.
- [12] D. A. Porter, K. E. Easterling, *Phase Transformation in Metals and Metal Alloys*, Van Nostrand Reinhold, New York 1981.

## Layer-by-Layer Assembly of Polythiophene

By Lei Zhai and Richard D. McCullough\*

The high conductivity, stability, and processibility of head-to-tail polythiophene has stimulated a lot of interest in the utilization of this fascinating material as active electronic elements in various thin film devices and sensors.<sup>[1,2]</sup> We have been interested in using a simple dipping method to facilitate

[\*] Prof. R. D. McCullough, L. Zhai  
Department of Chemistry, Carnegie Mellon University  
4400 Fifth Avenue, Pittsburgh, PA 15213 (USA)  
E-mail: rm5g@andrew.cmu.edu

the fabrication of regioregular polythiophene multilayer ultrathin films by electrostatic layer-by-layer self-assembly. Layer-by-layer self-assembly can provide easy control over the thickness of ultrathin film<sup>[3]</sup> and allow for the easy fabrication of nanoscale devices. Electrostatic layer-by-layer self-assembly was first introduced by Decher as a simple, versatile, and effective technique for the fabrication of ultrathin organic multilayer films.<sup>[4]</sup> This method involves sequential adsorption of polyanions and polycations on charged surface. The potential utility of this approach has also been exploited by Rubner<sup>[5]</sup> and other groups using a variety of important polymeric materials. This method has been applied to the assembly of conjugated polymers,<sup>[5]</sup> DNA,<sup>[6]</sup> protein,<sup>[7]</sup> and nanoparticles<sup>[8]</sup> in order to form layer-by-layer structures. A polythiophene polyelectrolyte multilayer was reported recently by Lukkari et al.<sup>[9]</sup> In their report, electronically conducting polyanions and polycations based on poly(thiophene alkoxy) derivatives were synthesized by using anhydrous FeCl<sub>3</sub> in dry chloroform, which resulted in a quite low conductivity ( $6.2 \times 10^{-4} \text{ S cm}^{-1}$ ) due to the low regioregularity of polymers. In this article, we provide the first fabrication of layer-by-layer self-assembly based on regioregular polythiophene, leading to structurally ordered nano-layered sheets of conducting polymers exhibiting electrical conductivities of  $0.04 \text{ S cm}^{-1}$  (Fig. 1).

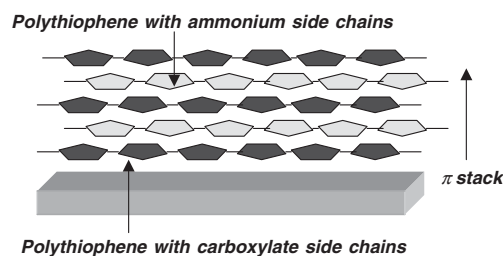
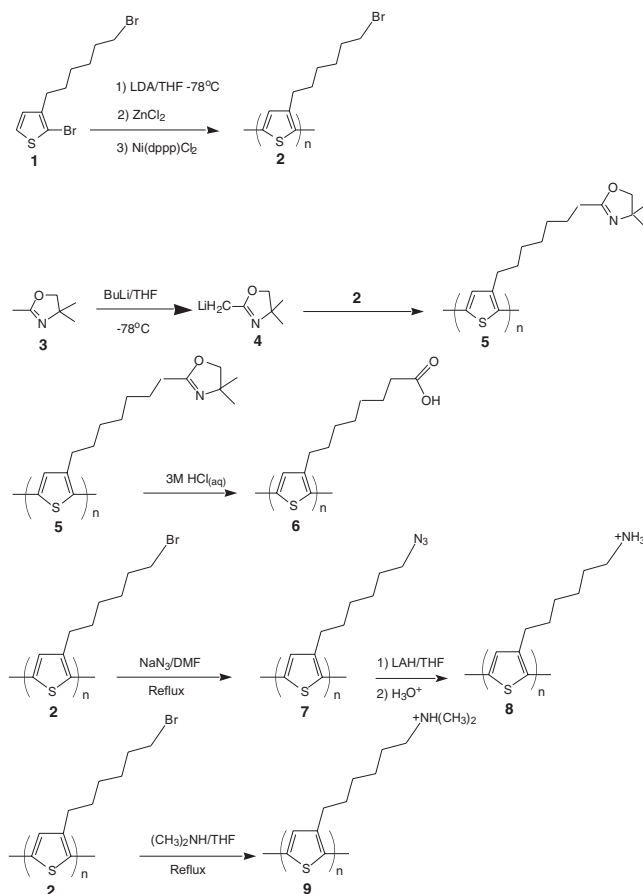


Fig. 1. Layer by layer self-assembly of regioregular polythiophene polyelectrolytes.

Polythiophenes bearing a carboxylic acid, a carboxylate, a primary amine, a primary ammonium, and a tertiary ammonium salt were employed to fabricate the layer-by-layer assembly. These polymers were synthesized by a post-polymerization functionalization method as shown in Scheme 1.

Poly(3-bromohexylthiophene) was synthesized from 5-bromo-3-hexylbromothiophene (**2**) using a method developed in our lab, see Experimental. Polymer **5** was prepared by treating poly(3-bromohexylthiophene) (**2**) with lithiated 2,4,4-trimethyl oxazoline at low temperature. As shown in Figure 2, <sup>1</sup>H NMR of polymer **5** proved that all bromide groups were converted to 2,4,4-trimethyl-2-oxazoline groups in post-polymerization functionalization since the triplet ( $\delta=3.40$ ) of the methylene group that was adjacent to bromine in Figure 2a disappeared completely and the requisite singlet ( $\delta=3.88$ ) (Fig. 2b) appeared in the NMR after the reaction is completed. The polymer **5** was also characterized by matrix-assisted laser desorption ionization time-of-flight mass spectrometry (MALDI-TOF MS). A mass of  $6 \text{ K} = 5566.4$  ( $\text{DP} = 20$ ) is observed and the observed mass difference between adjacent peaks corresponded to the molecular weight of mono-



Scheme 1. Synthesis of polythiophene derivatives by post-polymerization functionalization.

mer. Poly(3-octanic acid thiophene) (**6**) is made by the hydrolysis of polymer **5** under acidic conditions. Polymer **7** was synthesized by treating poly(3-bromohexyl thiophene) (**2**) with sodium azide in DMF. NMR characterization shows that the methylene triplet at 3.40 ppm (Fig. 2a) shifted to 3.25 (Fig. 2c), indicating that the substitution was complete. The reduction of polymer **7**, followed by acidic work-up led to ammonium-substituted polythiophene (**8**). Layer-by-layer conducting polymer self-assembly (Fig. 1) was accomplished by a simple dipping procedure providing electrostatically self-assembled ultra-thin films of carboxylate derivatives of regioregular polythiophene and ammonium derivatives of regioregular polythiophene. Layer-by-layer self-assembly was accomplished on both treated glass and gold-coated glass substrates. Glass slides were cleaned with sulfuric acid/hydrogen peroxide mixtures, rinsed with water, and dried. The clean slides were then treated with 5% (v/v) (3-aminopropyl)trimethoxysilane in anhydrous octane at 105 °C for 1 h. The amine-functionalized slides were washed with hexane and dried. The slides were then dipped in a DMF solution of a carboxylate or a carboxylic acid polythiophene, rinsed, and dried, and then dipped in a DMF/water solution of ammonium polythiophene. Repeating this simple procedure can produce multilayers of 40 bilayers or greater.

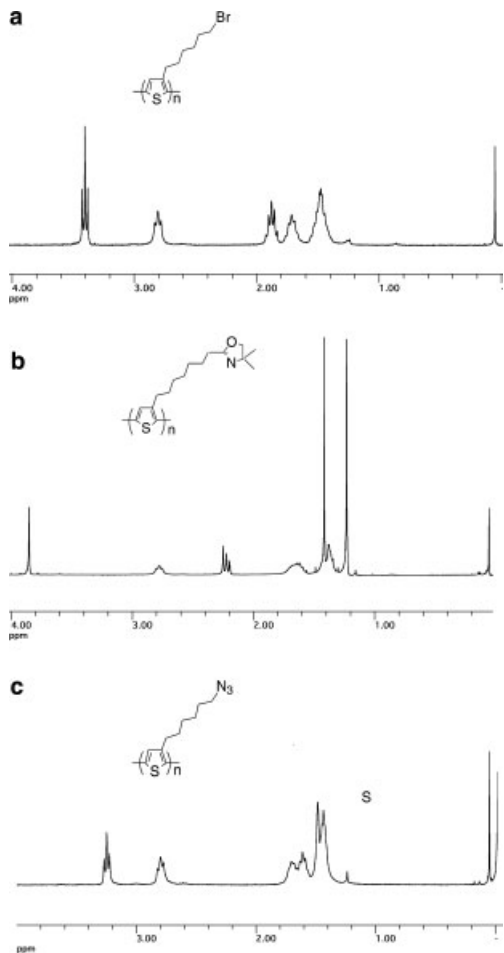


Fig. 2. NMR comparison of polythiophene after functionalization.

The UV-vis absorption spectra generated during the fabrication of multilayer thin films of these polythiophene derivatives indicated that the deposition process was completely reproducible from run to run. The linear relationship of the UV-vis absorption spectra demonstrated by a poly(3-octanic acid thiophene)/poly(hexylammonium thiophene) (**6/8**) multilayer system (Fig. 3) clearly indicated that each layer deposited contributes an equal amount of material to the thin film. It was found that high molecular weight polythiophene ( $M_n=15\,000$  from gel permeation chromatography (GPC)) could be readily manipulated into multilayer thin films while low molecular weight polythiophenes ( $M_n=3000$ ) failed to fabricate multilayer structures. Perhaps the reduction in cooperative binding reduces the possibility that the oligomeric thiophene form multilayers.

Poly(3-octanic acid thiophene)/poly(hexylammonium thiophene) (**6/8**) and poly(3-octanic acid thiophene)/poly-(3-(6-*N,N*-dimethylhexyl thiophene) (**6/9**) multilayer systems were fabricated under the same experimental conditions. The effect of the size of the side chains on the deposition density of polythiophene on each layer was studied by comparing the UV-vis absorption of each system. It was found that the absorption of the poly(3-octanic acid thiophene)/poly(3-(6-*N,N*-dimethylhex-

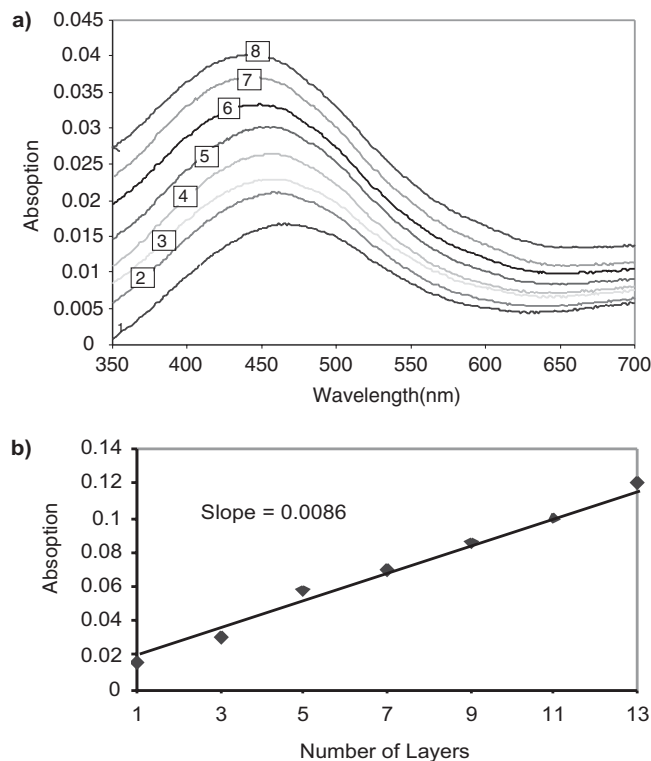


Fig. 3. a) Optical absorption vs. number of bilayers (indicated in boxes) deposited for poly(3-octanic acid thiophene)-poly(3-hexylammonium thiophene). b) Optical absorption vs. number of bilayers deposited for poly(3-octanic acid thiophene)-poly(3-hexylammonium thiophene).

yl thiophene) (**6/9**) system did not increase at the same rate as the more rapid absorption of poly(3-octanic acid thiophene)/poly(hexylammonium thiophene) (**6/8**) system as indicated by the difference in the slope of the absorption versus the number of bilayers deposited. The increase of steric hindrance of the side chains of poly(3-(6-*N,N*-dimethylhexyl)thiophene)s leads to a reduced conjugation as the layers increase relative to the less sterically encumbered poly(hexylammonium thiophene).

The conductivity of a 40 layer poly(3-octanic acid thiophene)/poly(hexylammonium thiophene) thin film, after oxidation with iodine vapor, was measured by a four-point probe technique. The thickness of the film was measured to be 16 nm via transmission electron microscopy (TEM), which indicates that each layer was 4 Å apart. This is roughly the ideal  $\pi$  stacking distance in stacked regioregular polythiophenes as determined by X-ray diffraction. This indicates that the polythiophene are  $\pi$ -stacked flat onto the surface. In poly(thiophene-3-acetic acid)/poly(allylamine) hydrochloride layer-by-layer self-assembled films, Rubner has also found that the polythiophenes lie preferentially in the plane of the substrate.<sup>[5a]</sup> In studies by Rubner,<sup>[5f]</sup> polyanilines and polypyrroles layer-by-layer assembled ultrathin films have been found to have conductivities of 1 and 40  $\text{S cm}^{-1}$ , respectively. However, the conductivities of the polythiophenes were not reported. The conductivity found in the regioregular polythiophenes reported here are 0.04  $\text{S cm}^{-1}$ , which was much higher than for regiorandom polythiophene multilayer sys-

tems ( $0.0006 \text{ S cm}^{-1}$ ) reported by Lukkari et al.<sup>[9]</sup> The regular polythiophene layer-by-layer assembled ultrathin films are much more organized than regiorandom polythiophene and simply have a higher electrical conductivity.

In conclusion, self-assembly by layer-by-layer deposition of polythiophene was successfully carried out using only polyanion and polycation dilute solutions of polythiophene. This investigation provides basic tools for the construction and the exploration of organized nano-layers of polythiophene.

## Experimental

**Synthesis of 3-bromohexylthiophene:** HPLC grade hexane dried over  $\text{CaH}_2$ , and dried THF were used as solvents. To a 500 mL 3-necked round bottom flask equipped with stirring equipment was added 3-bromothiophene (30 g, 0.18 mol) and 250 mL hexane was added via a syringe. The flask was chilled down to  $-40^\circ\text{C}$  and the solution was stirred for 10 min. *n*-BuLi (72 mL, 0.18 mol) was added dropwise via a syringe at this temperature. After stirring for 10 min, 15 mL THF was added dropwise via a syringe. The solution was stirred for 1 h, then the cooling bath was removed and the solution was allowed to warm to  $-10^\circ\text{C}$ . Dibromohexane (110 mL, 0.72 mol) was added in one portion and the solution was warmed to room temperature. The solution was stirred for 2 h at room temperature, then extracted with  $\text{Et}_2\text{O}$  ( $3 \times 20 \text{ mL}$ ) and organic extracts were washed with water ( $3 \times 20 \text{ mL}$ ). The organic layer was dried over anhydrous  $\text{MgSO}_4$  and the removal of solvent gave a crude product. The product was further purified by vacuum distillation.  $^1\text{H NMR}$  ( $\delta$ ,  $\text{CDCl}_3$ ): 7.24 (d, 1H), 6.92 (d, 1H), 3.40 (t, 2H), 2.64 (t, 2H), 1.86 (m, 2H), 1.65 (m, 2H), 1.5 (m, 2H), 1.2 (m, 2H). Elemental analysis [%]: C: 48.38 (calculated 48.59), H: 6.04 (calculated 6.12), Br: 32.32 (calculated 32.32)

**Synthesis of 2-bromo-3-bromohexylthiophene 1:** 3-bromohexyl-thiophene (27.39 g, 0.11 mol) was dissolved in a mixture of THF and acetic acid (1:1, v/v, 135 mL each) in a 500 mL one necked flask equipped for stirring. *n*-Bromosuccinimide (23.66 g, 0.13 mol) was added to the solution in one portion and the solution was stirred for 1 h. Then the solution was extracted with  $\text{Et}_2\text{O}$  ( $3 \times 50 \text{ mL}$ ) and the organic extracts were washed with water ( $3 \times 50 \text{ mL}$ ) and  $\text{NaHCO}_3$  (aq) ( $2 \times 50 \text{ mL}$ ). The organic layer was dried over anhydrous  $\text{MgSO}_4$  and the removal of solvent gave a crude product. Distillation at  $120^\circ\text{C}$  under 0.05 torr gave 25.2 g colorless 2-bromo-3-bromohexylthiophene.  $^1\text{H NMR}$  ( $\delta$ ,  $\text{CDCl}_3$ ): 7.18 (d, 1H), 6.78 (d, 1H), 3.40 (t, 2H), 2.58 (t, 2H), 1.87 (m, 2H), 1.61 (m, 2H), 1.51 (m, 2H), 1.39 (m, 2H). Elemental analysis [%]: C: 36.83 (calculated 36.83), H: 4.29 (calculated 4.33), S: 9.82 (calculated 9.83), Br: 49.07 (calculated 49.08).

**Synthesis of HT-poly(3-bromohexylthiophene) 2:** To a 3-necked 100 mL round bottom flask equipped for stirring was added dry diisopropylamine (12 mmol) and 25 mL freshly distilled THF was added via a syringe. The solution was cooled down to  $-70^\circ\text{C}$ . *n*-BuLi (4 mL, 10 mmol) was added via a syringe and the solution was stirred for 1.5 h. 2-bromo-3-hexylbromothiophene (3.26 g, 10 mmol) was added in one portion via a syringe. The mixture was stirred for 2 h at  $-78^\circ\text{C}$ .  $\text{ZnCl}_2$  (1.37 g, 10 mmol) was added in one portion and the reaction was stirred until  $\text{ZnCl}_2$  was dissolved. The cooling bath was removed and the mixture was warmed up to  $-5^\circ\text{C}$ .  $\text{Ni}(\text{dppp})\text{Cl}_2$  (dppp=1,3-diphenylphosphinopropane) (27 mg, 0.05 mmol) was added. The mixture was warmed to room temperature, stirred for 20 min and quenched with methanol. The solid polymer was washed with methanol by using a Soxhlet extractor. The polymer then was dissolved by Soxhlet extraction with chloroform, the chloroform was removed, and the residue was dried under vacuum to yield 1.51 g of 98 % head-to-tail coupled poly(3-bromohexylthiophene) with 61 % yield.  $^1\text{H NMR}$  ( $\delta$ ,  $\text{CDCl}_3$ ): 6.95 (s, 1H), 3.40 (t, 2H), 2.80 (t, 2H), 1.88 (m, 2H), 1.70 (m, 2H), 1.51 (m, 4H). Elemental analysis [%]: C: 49.02 (calculated 48.9), H: 5.43 (calculated 5.3), S: 13.11 (calculated 13.1), Br: 32.74 (calculated 32.74).  $M_n=14630$  (by GPC).

**Synthesis of 2,5-Poly(3-(2-(4,4-dimethylloxazolin-2-yl)-heptyl)thiophene) 5:** To a 3-necked 100 mL round bottom flask was added freshly dried 2,4,4-trimethylloxazoline (2.26 g, 20 mmol) and 30 mL dry THF was added via syringe. The flask was cooled to  $-70^\circ\text{C}$  and the solution was stirred for 10 min. *n*-BuLi (7.2 mL, 18 mmol) was added dropwise via syringe to the solution. The solution was stirred for 2 h. Poly(3-bromohexylthiophene) (0.49 g, 2 mmol) was dissolved in 30 mL dry THF. The polymer solution was transferred to oxazoline lithium salt solution via cannula and the addition was completed in 30 s. The cooling bath was removed, the mixture was stirred for 1 h and quenched in hex-

ane. The solid polymer was washed with hexane by using a Soxhlet extractor. 519 mg polymer was obtained with 93 % yield.  $^1\text{H NMR}$  ( $\delta$ ,  $\text{CDCl}_3$ ): 6.95 (s, 1H), 3.88 (s, 2H), 2.80 (t, 2H), 2.25 (t, 2H), 1.70 (m, 2H), 1.40 (m, 8H), 1.22 (s, 6H).  $M_n=16610$  (by GPC).

**Synthesis of HT-2,5-poly(3-octanic acid thiophene) 6:** A sample of 2,5-poly(3-(2-(4,4-dimethylloxazolin-2-yl)-heptyl)thiophene) (278 mg, 1 mmol) was dissolved in 3M HCl (60 mL) in a 300 mL one neck round bottom flask and heated to reflux for 12 h. The solid was filtered, rinsed with  $\text{H}_2\text{O}$ , and dried to recover the product in 86 % yield.  $^1\text{H NMR}$  ( $\delta$ , pyridine): 7.09 (s, 1H), 2.67 (t, 2H), 2.20 (t, 2H), 1.49 (m, 4H), 1.09 (m, 6H). Elemental analysis [%]: C=62.16 (calculated 64.2), H=7.27 (calculated 7.14).  $M_n=15200$  (by GPC).

**Synthesis of HT-2,5-poly(3-hexylazide thiophene) 7:** To a 3-necked 100 mL round bottom flask equipped for stirring was added poly(3-bromohexyl thiophene) (490 mg, 2 mmol), 30 mL DMF was added and the solution was heated to reflux. sodium azide (1.3 g, 20 mmol) was added in one portion and the mixture was stirred overnight at reflux temperature of DMF. The reaction was quenched in methanol. The solid polymer was washed with methanol by using a Soxhlet extractor. 330 mg polymer was obtained with 80 % yield.  $^1\text{H NMR}$  ( $\delta$ ,  $\text{CDCl}_3$ ): 6.95 (s, 1H), 3.25 (t, 2H), 2.80 (t, 2H), 1.51 (m, 8H).  $M_n=14590$  (by GPC).

**Synthesis of HT-2,5-poly(3-hexylamine thiophene) 8:** To a 3-necked 100 mL round bottom flask equipped for stirring was added poly(3-hexylazide thiophene) (400 mg, 2 mmol), 30 mL dry THF was added via syringe. Lithium aluminum hydride in THF solution (2 mL, 4 mmol) was injected via syringe and the solution was stirred for 30 min, and quenched in water. The precipitate was filtered and dried under vacuum, and 340 mg polymer was obtained with 94 % yield.  $^1\text{H NMR}$  ( $\delta$ , tetrahydrofuran): 6.95 (s, 1H), 2.80 (t, 2H), 2.52 (t, 2H), 1.32 (m, 8H).  $M_n=14320$  (by GPC).

**Synthesis of HT-2,5-poly(3-(6-*N,N*-dimethylhexylammonium thiophene) 9:** To a 3-necked 100 mL round bottom flask equipped for stirring was added poly(3-bromohexyl thiophene) (490 g, 2 mmol), 30 mL dry THF was added via syringe. dimethylamine in THF solution (20 mL, 30 mmol) was added via syringe and the mixture was stirred at  $60^\circ\text{C}$  overnight. The mixture was dissolved in methanol/water(1:1, v/v) and  $\text{KCO}_3$  was added. The precipitate was dissolved in chloroform and the solution was washed with water ( $3 \times$ ) followed by evaporation of the solvent. 313 mg polymer was obtained with 73 % yield.  $M_n=15630$  (by GPC).

**Substrate Preparation:** The glass slides were cleaned with a solution of three volumes of  $\text{H}_2\text{SO}_4$  and one volume of 30 %  $\text{H}_2\text{O}_2$  for 30 min and washed with distilled water. After drying, the slides were treated with 5 % (v/v) (3-amino-propyl)trimethoxysilane(Acros) in anhydrous octane at  $105^\circ\text{C}$  for 1 h. The amine-functionalized slides were washed with hexane and dried.

**Multilayer Deposition on Glass: Poly(3-octanic acid thiophene)/poly(3-hexylammonium thiophene) System:** Poly(3-octanic acid thiophene) (42 mg, 0.2 mmol) was dissolved in 20 mL DMF and poly(3-hexylammonium thiophene) (36 mg, 0.2 mmol) was dissolved in 1:1 DMF/water to make 0.01 M solutions. The glass slide was dipped into the solution of polythiophene bearing acid side chains for 30 min, rinsed with DMF, and dried in air. The slide was then dipped into polycation solution for 30 min followed by washing and drying. Multilayer thin films were prepared by simply repeating this basic bilayer deposition process.

**Poly(3-octanic acid thiophene)/poly(3-(6-*N,N*-dimethyl)hexyl thiophene) System:** Poly(3-octanic acid thiophene) (42 mg, 0.2 mmol) was dissolved in 20 mL DMF and poly(3-hexylammonium thiophene) (41 mg, 0.2 mmol) was dissolved in 20 mL 1:1 DMF/water to make 0.01 M solutions. The glass slide was dipped into the solution of polythiophene bearing acid side chains for 30 min, rinsed with DMF, and dried with air. The slide was then dipped into polycation solution for 30 min, followed by washing and drying. Multilayer thin films were prepared by simply repeating this basic bilayer deposition process.

**Poly(3-potassiumoctate thiophene)/poly(3-hexylammoniumacetate thiophene) System:** Poly(3-octanic acid thiophene) (21 mg, 0.1 mmol) was dissolved in 10 mL 1 M KOH(aq) and poly(3-hexylamine thiophene) (18 mg, 0.1 mmol) was dissolved 10 mL 1 M acetic acid(aq). The glass slide was dipped into the polyanion solution for 20 min, rinsed with water, and dried in air. The slide was then dipped into polycation solution for 20 min followed by washing and drying. Multilayer thin films were prepared by simply repeating this basic bilayer deposition process.

**Multilayer Deposition on Gold Surface:** 80 nm thick gold was sputter coated on the glass slide by Pelco SC-6 sputter coater, and the slide was treated by 0.5 M 2-aminoethanethiol hydrochloride in ethanol overnight. The slide was washed with anhydrous ethanol and dried with air. The slide was dipped into the solution of polythiophene bearing acid side chains for 30 min, rinsed with DMF, and dried with air, followed by dipping into polycation solution for 30 min, followed by washing and drying. Multilayer thin films were prepared by simply repeating this basic bilayer deposition process.

**Measurement of Conductivity:** The resistance of the multilayer was measured by a four-point probe method and the thickness of the multilayer was measured by TEM.

Received: January 28, 2002  
Final version: March 28, 2002

- [1] J. H. Schön, A. Dodabalapur, Z. Bao, C. Kloc, O. Schenker, B. Batlogg, *Nature* **2001**, *410*, 189.
- [2] Q. Zhou, T. M. Swager, *J. Am. Chem. Soc.* **1995**, *117*, 12593.
- [3] J. R. Heflin, C. Figura, D. Marciu, Y. Liu, R. O. Claus, *Appl. Phys. Lett.* **1999**, *74*, 495.
- [4] G. Decher, *Science* **1997**, *277*, 1232.
- [5] a) M. Ferreira, M. F. Rubner, *Macromolecules* **1995**, *28*, 7107. b) J. D. Mendelsohn, C. J. Barrett, V. V. Chan, A. J. Pal, A. M. Mayes, M. F. Rubner, *Langmuir* **2000**, *16*, 5017. c) S. S. Shiratori, M. F. Rubner, *Macromolecules* **2000**, *33*, 4213. d) A. Wu, D. Yoo, J.-K. Lee, M. F. Rubner, *J. Am. Chem. Soc.* **1999**, *121*, 4883. e) S. Joly, R. Kane, L. Radzilowski, T. Wang, A. Wu, R. E. Cohen, E. L. Thomas, M. F. Rubner, *Langmuir* **2000**, *16*, 1354. f) J. H. Cheung, A. F. Fou, M. F. Rubner, *Thin Solid Films* **1994**, *244*, 985.
- [6] Y. Lvov, G. Decher, G. Sukhorukov, *Macromolecules* **1993**, *26*, 5396.
- [7] Y. Lvov, K. Ariga, I. Ichinose, T. Kanitake, *J. Am. Chem. Soc.* **1995**, *117*, 6117.
- [8] J. W. Ostrander, A. A. Mamedov, N. A. Kotov, *J. Am. Chem. Soc.* **2001**, *123*, 1102.
- [9] J. Lukkari, J. Paukkunen, N. Kocharova, N. Kankare, *J. Am. Chem. Soc.* **2001**, *123*, 6083.

## Development of Metal Oxide Nanoparticles with High Stability Against Particle Growth Using a Metastable Solid Solution\*\*

By Edson R. Leite,\* Adeilton P. Maciel, Ingrid T. Weber, Paulo N. Lisboa-Filho, Elson Longo, C. O. Paiva-Santos, A. V. C. Andrade, C. A. Pakoscimas, Y. Maniette, and Wido H. Schreiner

Several technological and scientific phenomena in materials science are directly related to particle size. In some cases, as in catalyst materials and gas sensors, it is desirable to produce materials with nanometer-scale structures to obtain specific properties. However, it is very difficult to maintain the nanometer-scale structure of a material when it is subjected to heat treatments. Heat-treatment steps are fundamental to achieve an optimal combination of mechanical, catalytic, and electronic properties upon application. Therefore, an important area of research is the development of new synthesis methods or processes to control or improve the stability of nanostructured materials against particle (crystal) growth during heat-treatment steps or during their use at high temperatures. Such research may lead to catalytic and electronic materials (such as gas sensors)

with superior performance. We report, herein, on a new approach to improve the thermal stability of nanostructured metal oxides, more specifically tin oxide, against particle growth. This approach is based on the reduction of the particle growth rate at high temperatures through the formation of a metastable solid solution between SnO<sub>2</sub> and dopants such as rare earth oxides (Y<sub>2</sub>O<sub>3</sub>, La<sub>2</sub>O<sub>3</sub>, and CeO<sub>2</sub>). Tin oxide (SnO<sub>2</sub>), a semiconductor, was chosen to test this approach because it is a material of considerable technological importance with interesting electronic and catalytic properties.<sup>[1]</sup>

Considering that particle growth is controlled by the motion of the boundaries between particles,<sup>[2]</sup> one can assume that the mean boundary velocity,  $v$ , is proportional to the thermodynamic driving force,  $\Delta F$ , applied to it

$$v = M\Delta F \quad (1)$$

where  $M$  is the particle-boundary mobility, which depends on the mechanism of diffusion (a kinetic parameter in Eq. 1). Thus, two distinct approaches can be used to prevent particle growth, i.e., a slow down of the growth kinetics by reduction of  $\Delta F$  or a reduction of particle boundary mobility. Wu et al.<sup>[3]</sup> recently reported on the inhibition of particle growth upon firing hydrous transition metal oxide gels by replacing the surface hydroxyl groups before firing with another functional group. This can produce small secondary-phase particles that act as pinning sites for the particle boundaries at high temperatures. Nayral et al.<sup>[4]</sup> proposed an interesting route to synthesize nanometer-size SnO<sub>2</sub> particles, based on the oxidation of Sn nanoparticles. These authors controlled the particle growth through the formation of an external oxide layer. Leite et al.,<sup>[5]</sup> on the other hand, suggested that, during the synthesis of SnO<sub>2</sub>, particle growth can be controlled by the addition of Nb<sub>2</sub>O<sub>5</sub>, which will segregate and contribute toward its inhibition. This may produce two beneficial effects. The first is the solute drag, which causes a decrease in particle mobility.<sup>[6]</sup> The second is a reduction of the driving force,  $\Delta F$ . Experimental and theoretical evidences in metal systems have demonstrated that the decrease in  $\Delta F$  may be substantial, particularly in metastable solid solution systems.<sup>[7]</sup> In both cases, i.e., solute drag and reduction of the driving force, the formation of a metastable solid solution is fundamental to the development of a segregation layer of foreign cations in the particle surface.

Since the idea is to form a metastable solid solution, whatever synthetic chemical method is used must provide the possibility of creating metastable phases. The polymeric precursor technique is a well-known soft chemical method<sup>[8]</sup> that can process both amorphous<sup>[9]</sup> and crystalline metastable phases.<sup>[10]</sup> Thus, we employed this method to process doped and undoped SnO<sub>2</sub> with different dopants. In this study the dopant concentration was fixed at 5 mol-%. Dopant concentrations higher than 5 mol-% did not show any improvement in the control of the SnO<sub>2</sub> particle size. Further details of this method have been published before.<sup>[5]</sup>

[\*] Dr. E. R. Leite, A. P. Maciel, I. T. Weber, Dr. P. N. Lisboa-Filho, Dr. E. Longo CMDMC—LIEC-DQ-UFSCar São Carlos, SP, CEP 13565-905 (Brazil) E-mail: derl@power.ufscar.br

Dr. C. O. Paiva-Santos, A. V. C. Andrade, Dr. C. A. Pakoscimas, Dr. Y. Maniette IQ-UNESP- Araraquara SP, CEP 14800-900 (Brazil) Dr. W. H. Schreiner LSI- Depto. de Física -UFPR Curitiba, PR CEP 81531-990 (Brazil)

[\*\*] Financial support by FAPESP, CNPq, and CAPES is gratefully acknowledged.